

Studies of Improved Electron Confinement on NSTX

D. Stutman 1), K. W. Hill 2), S. M. Kaye 2), M. H. Redi 2), E. J. Synakowski 2), M. G. Bell 2), R. E. Bell 2), C. Bourdelle 3), W. Dorland 4), M. Finkenthal 1), S. Kubota 5), B. P. LeBlanc 2), F. Levinton 6), J. E. Menard 2), D. R. Mikkelsen 2), K. Tritz 1), and the NSTX Team

- 1) Johns Hopkins University, Baltimore, MD, USA
- 2) Princeton Plasma Physics Laboratory, Princeton, NJ, USA
- 3) Association Euratom-CEA, Cadarache, France
- 4) University of Maryland, College Park, MD, USA
- 5) University of California, Los Angeles, CA, USA
- 6) Nova Photonics, Princeton, NJ, USA

e-mail contact of main author: stutman@pppl.gov

Abstract. A regime of improved electron confinement is observed in low density NSTX (National Spherical Torus Experiment) discharges heated by early beam injection. We used this regime to perform experiments in which the role of the current profile on thermal transport was investigated. Variations in the magnetic shear profile were produced by changing the current ramp rate and onset of neutral beam heating. A steep electron temperature gradient and local minimum in the electron thermal diffusivity are observed at early times in plasmas with the fastest current ramp and earliest beam injection. In addition, a localized region of reduced ion transport is observed at larger radii. Measurements of double-tearing MHD activity and current diffusion calculations point to the existence of negative magnetic shear in the core of these plasmas. Plasmas with slower current ramp and delayed beam onset that are estimated to have flat and monotonic q-profiles do not exhibit such regions of reduced transport. The results are discussed in the light of the initial linear microstability assessment of these plasmas, which suggests that the growth rate of TEM and ETG range instabilities is reduced by negative magnetic shear in the T_e gradient region.

1. Introduction.

Understanding electron thermal transport is a major challenge for all toroidal fusion devices. Early predictions of suppression of ion scale instabilities in the spherical torus are supported by initial observations on NSTX of ion thermal and particle transport near neoclassical levels [1,2]. However, electron thermal transport rates reported thus far are high [1], raising the possibility that a different class of instabilities may be driving the electron thermal channel. This separation might nevertheless provide an opportunity to elucidate on NSTX more general aspects of electron transport.

The typical transport picture in an intermediate density ($\langle n_e \rangle \approx 4 \cdot 10^{13} \text{ cm}^{-3}$), neutral beam heated L-mode discharge in NSTX is illustrated in Fig. 1a. The core ion temperature T_i , exceeds the electron temperature T_e , by about 30%, although the beam ions preferentially heat the electrons [1]. This reflects in the electron thermal diffusivity χ_e , being much higher than the ion one, χ_i . The latter, together with the impurity diffusivity D_{imp} , fall in the range of the neoclassical predictions [2]. A similar situation occurs in high power H-modes, where the central T_e does not increase as compared to the L-mode, but rather the T_e profile broadens (Fig. 1b). Even increasing the heating power by 50% does not change the T_e profile by much, which is reflected in an increase in χ_e that effectively offsets the additional heating. One can also note that in such discharges the core χ_e often reaches several tens of m^2/s . Comparable trends are observed in the MAST spherical torus [3]. Due to the comparatively low ion thermal and particle diffusivity however, the energy confinement time τ_E , in beam heated NSTX plasmas often exceeds the conventional aspect ratio tokamak scaling [4]. High plasma

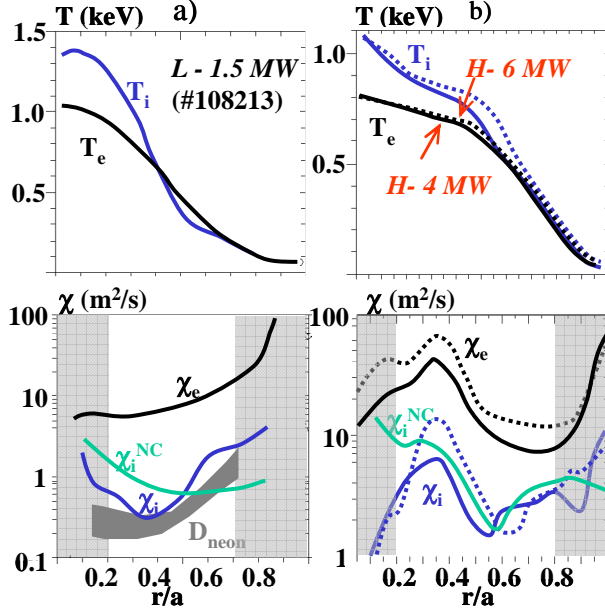


FIG.1 a) $T_{e,i}$ and $\chi_{e,i}$ profiles in intermediate n_e L-mode (#108213, 1MA, 4.5 kG, $t=0.3s$). Also shown the NCLASS χ_i and the Ne diffusivity. b) $T_{e,i}$ and $\chi_{e,i}$ profiles for otherwise identical H-modes heated by 4 and 6 MW beams, respectively. (#112570 and #112581, 1 MA, 4.5 kG, $t=0.55s$).

varied the plasma current ramp-rate and beam timing in low density ($\langle n_e \rangle \approx 2 \cdot 10^{13} \text{ cm}^{-3}$), fixed beam power (2MW at $R_{\text{tan}} \approx 60 \text{ cm}$) discharges. Double null diverted, L-modes discharges having 1 MA current, 4.5 kG toroidal field, $\kappa \approx 2$, and $\delta \approx 0.6-0.7$ were used as a base line scenario. Time histories obtained at low n_e with fast current ramp and early beam injection (shot #112989, 6.5 MA/s, $t_{\text{beam,on}} \approx 0.05 \text{ s}$) are compared with those obtained with slow current ramp and late beam injection (shot #112996, 4 MA/s, $t_{\text{beam,on}} \approx 0.12 \text{ s}$) in Fig. 2a. The plasma profiles are also compared in Fig. 2. We choose to compare the profiles at about equal times after the beam turn-on ($t_1 \approx 0.19$ for 112989 and $t_2 \approx 0.25 \text{ s}$ for 112996). There are two reasons for this choice. First, it minimizes potential differences arising from beam slowing down effects. Second, and more importantly, at these times the plasma is spun up to comparable velocities, thus eliminating the effect of differences in rotation on transport and enabling the comparison of the effects of magnetic shear.

The time histories show that in both cases T_{e0} increases to $\approx 1.5 \text{ keV}$ after 0.12-0.15 s of beam heating. The sudden T_{e0} decrease occurring in both plasmas after the initial rise ($t \approx 0.22 \text{ s}$ and $\approx 0.27 \text{ s}$, respectively) is associated with large reconnection or transport events, as discussed below. Before these times, the USXR data indicate that in both cases the plasma core is free from large reconnection events. A faint *off-axis* reconnection is identified in the fast ramp shot 112989 around 0.182 s. Also, a high- m mode appears at mid-radius in this shot, shortly before the large reconnection at $t \approx 0.22 \text{ s}$. This mode is likely causing the plateau in the rotation profile at $r/a \approx 0.4-0.55$ in Fig. 2b. The Mirnov coil data at t_1 and t_2 show only high frequency (TAE range), high- n (3-5 in 112989 and 2-4 in 112996) MHD activity in both discharges.

Although the central electron and ion temperatures are comparable at the chosen times, the gradient in their profiles is however quite different. As seen both in the raw data in Fig. 2a and the TRANSP mapped profiles in Fig. 2b [4], the T_e profile of the fast ramp case has a steeper gradient around mid-radius. It is possible that the gradient is in reality even stronger. The experimental resolution is limited by the several cm spacing of the Thomson

rotation velocities also point to good momentum confinement [1]. This transport picture is in contrast with the conventional tokamak ordering, where generally $\chi_e \approx \chi_i \geq D_{\text{imp}}$.

A regime of different electron (and ion) transport is nevertheless observed in low density NSTX discharges heated by early beam injection, where the core T_e and its gradient can rapidly increase, indicating the presence of an internal transport barrier. Magnetic diffusion calculations and ultrasoft x-ray (USXR) imaging suggest magnetic shear reversal in these plasmas. Since this low density regime has quite different electron confinement compared to the ‘standard’ NSTX plasma, we used it to study current profile effects on electron transport.

2. Experiments

In order to change the q -profile we

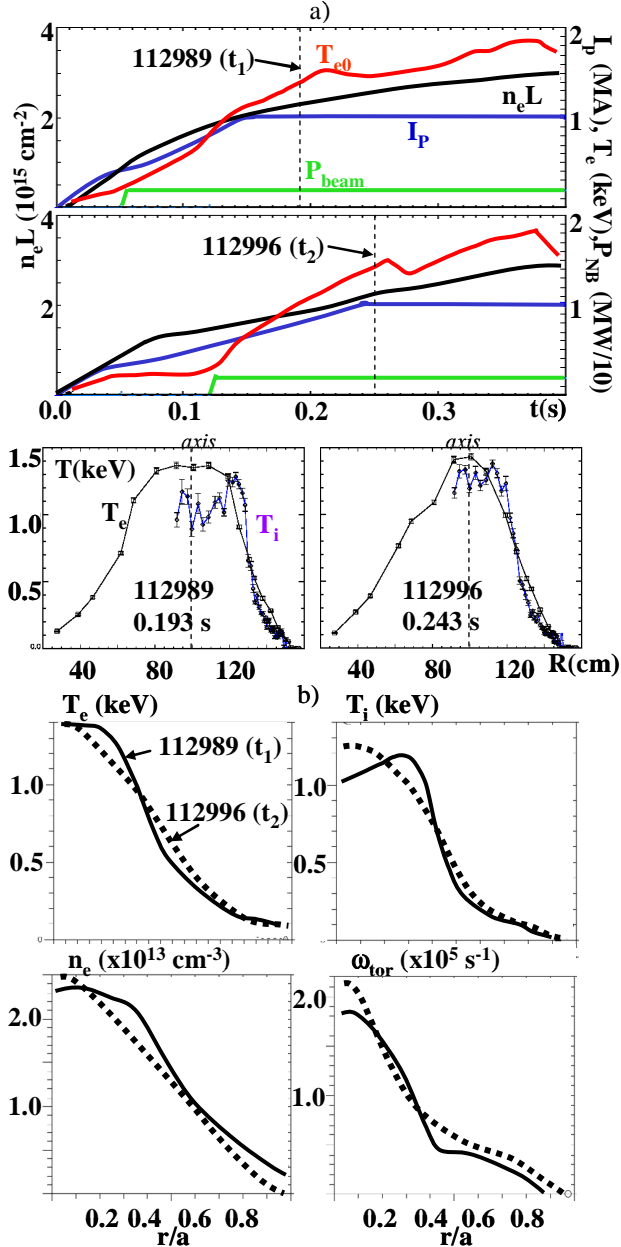


FIG. 2 a) I_p , P_{beam} , T_{e0} and line density in fast ramp, early injection (#112989) and slow ramp, late injection (#112996) discharges. Also shown the raw $T_{e,i}$ profiles at the indicated times. b) Plasma profiles as a function of minor radius ($\sqrt{\Phi/\Phi_a}$) at the times of comparison.

that by $t \approx 0.36$ s in shot 112989 the electron and ion barriers have ‘weakened’ into a broad region of χ_e , χ_i around a few m^2/s , while in shot 112996 both χ_e and χ_i decrease towards similar values. The overall confinement is good in this regime ($\tau_E \approx 70$ – 75 ms in both shots at 0.36 s, reaching $\tau_E \approx 95$ – 100 ms in 112989 at $t \approx 0.43$ s).

The main question arising from the above results is what causes the early differences in electron (and ion) transport between the two cases. While the q -profile is a prime candidate, the MSE internal measurement of the magnetic pitch profile was not available in these experiments. The analysis of soft X-ray and magnetic fluctuations points however to a reversed q -profile in the fast ramp, early injection discharges. Both at earlier and later times in

scattering points in the core. The T_i and n_e profiles also show increased gradients. An interesting occurrence is the flattening of the T_e profile inside $r/a \approx 0.2$, despite the absence of MHD reconnections. Within the uncertainty illustrated by the error bars in Fig. 2a, the central T_i profile is hollow in 112989. The angular rotation profiles are relatively similar as planned, with both profiles showing a shallow gradient up to $r/a \approx 0.4$ (with a plateau in 112989), followed by a rapid increase to high rotation in the core region. The fast ramp case has a somewhat broader rotation profile however.

The TRANSP power balance analysis of the two low n_e discharges indicates large differences (Fig. 3). The shaded areas delineate regions where there are large uncertainties in the inferred transport coefficients [1,4]. In the fast ramp case a strong reduction in χ_e is seen between $r/a \approx 0.3$ – 0.45 , indicative of an electron ITB. There is also a strong reduction in χ_i towards neoclassical values between $r/a \approx 0.4$ – 0.5 , indicating also an ion ITB. In the slow ramp case on the other hand, χ_e decreases rather monotonically up to $r/a \approx 0.25$, while χ_i stays above several m^2/s at all radii. The confinement times also differ, with $\tau_E \approx 70$ ms at t_1 in the fast ramp case and $\tau_E \approx 40$ ms at t_2 in the slow ramp case.

At later times however ($t \geq 0.35$ s), the central T_e values again become very similar in the two discharges (Fig. 2a). The same holds for the overall T_e , T_i , n_e , and rotation profiles. The transport picture is illustrated in Fig. 4, indicating

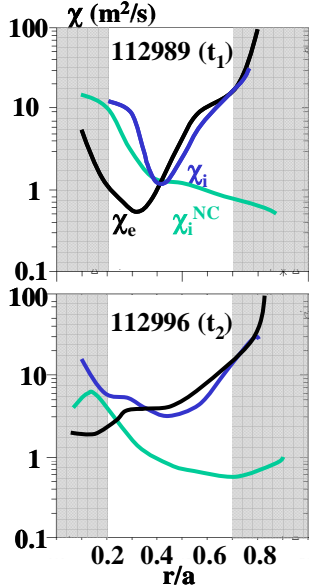


FIG. 3 TRANSP $\chi_{e,i}$ at the times of comparison.

ramp discharges. Simulations with different mapping options for the measured plasma profiles produce a band of q -profiles, as shown in Fig. 6a. A consistent feature in these predictions is a large difference between the *shape* of the q -profiles in the shots of interest. The fast ramp case has large negative shear at the time t_1 when the electron barrier is formed, while the slow ramp case has flat or only slightly reversed q -profile at t_2 .

Concerning magnetic indications for a hollow current profile, the plasma inductance in shot 112989 is relatively high, $l_i \approx 0.9$ around t_1 . Nevertheless similar, or higher inductance is measured in the discharges where the MSE diagnostic confirms the q -profile reversal.

3. Discussion

The present experiments were motivated primarily by the question whether the current profile can directly influence electron transport on NSTX. To this end we tried producing discharges with different q -profiles, while having other parameters potentially important for

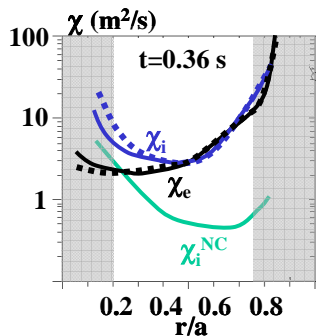


FIG. 4 $\chi_{e,i}$ and χ_{i}^{NC} in shots 112989 and 112996 (dotted lines) at $t \approx 0.36$ s.

these shots, the T_e sensitive USXR profiles display faint, off-axis sawtooth-like crashes, in which only the outer plasma emission is involved (Fig. 5a left). Similar MHD behavior has been seen in plasmas in which the MSE diagnostic was operating and confirmed negative shear (Fig. 5a right). ‘Two-color’ modeling of the USXR profiles as in ref. [5] shows that these sawteeth are associated with off-axis T_e crashes, as observed e.g., in TFTR reversed shear plasmas [6]. Also, associated with these crashes, two 1/1 coherent modes appear at distinct radii, indicative of the existence of two $q=1$ surfaces in the plasma (Fig. 5b). Finally, in discharges that do not exhibit strong reconnections before $q \approx 1$ is reached, a direct comparison with the q -profile predicted by TRANSP assuming magnetic diffusion can be made [4]. Using the location of the two 1/1 modes and off-axis T_e crashes to pinpoint the two $q=1$ surfaces and a 3/2 mode to localize the $q=1.5$ surface, an approximate q -profile is derived from the USXR data that corroborates the TRANSP prediction (Fig. 5c).

TRANSP modeling was further used to assess the differences in the current distribution between the fast and slow

ramp discharges. Simulations with different mapping options for the measured plasma profiles produce a band of q -profiles, as shown in Fig. 6a. A consistent feature in these predictions is a large difference between the *shape* of the q -profiles in the shots of interest. The fast ramp case has large negative shear at the time t_1 when the electron barrier is formed, while the slow ramp case has flat or only slightly reversed q -profile at t_2 .

Concerning magnetic indications for a hollow current profile, the plasma inductance in shot 112989 is relatively high, $l_i \approx 0.9$ around t_1 . Nevertheless similar, or higher inductance is measured in the discharges where the MSE diagnostic confirms the q -profile reversal.

The present experiments were motivated primarily by the question whether the current profile can directly influence electron transport on NSTX. To this end we tried producing discharges with different q -profiles, while having other parameters potentially important for transport, like $\mathbf{E} \times \mathbf{B}$ shearing rates, T_i/T_e ratio and β relatively similar. The $\mathbf{E} \times \mathbf{B}$ shearing rates computed by TRANSP in the two discharges using the un-smoothed, outboard plasma profiles are plotted in Fig. 6b. Although there are uncertainties in the absolute values, the relative comparison is meaningful. This comparison shows that, primarily as a consequence of the comparable rotation profiles, the two plasmas have quite similar (and large) $\mathbf{E} \times \mathbf{B}$ shearing rates over much of the radius. The T_i/T_e ratio is also comparable for the two shots (Fig. 2), while β is around 8% in both cases at the times of comparison. This leaves the estimated difference in the q -profiles as the likely cause for the observed differences in transport.

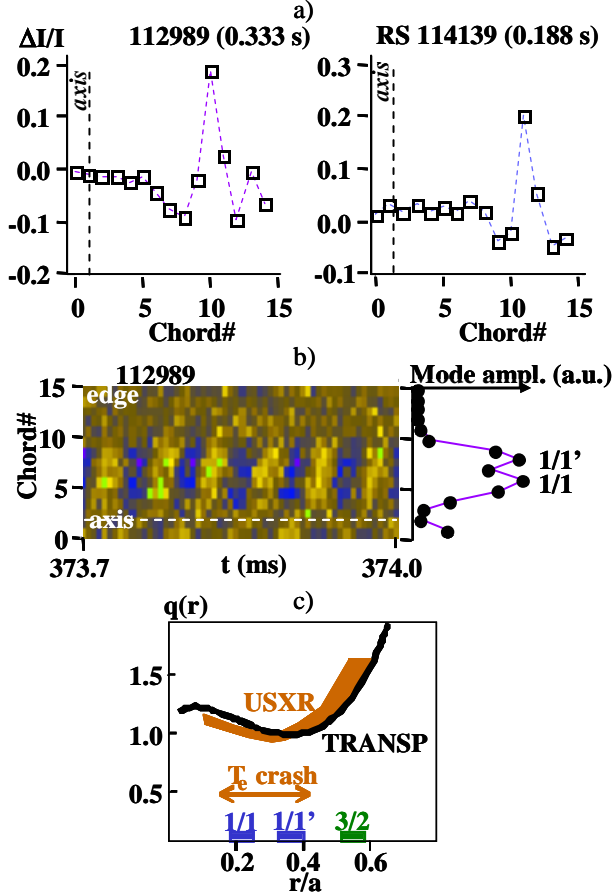


FIG. 5 a) Change in T_e sensitive ($E > 1.4$ keV) USXR profiles ($I_{\text{after}} - I_{\text{before}} / I_{\text{before}}$), measured at off-axis sawtooth crashes in shot 112989, and in shot confirmed by MSE to have shear reversal. The diode array views the upper plasma half along 15 chords. b) Coherent modes seen by the same array in the fast ramp shot. The graph shows the USXR perturbation amplitude at the mode frequency. c) Comparison between the USXR $q(r)$ estimate and the TRANSP prediction (#108918, 5 MA/s, 1 MA, 4.5 kG, $t \approx 0.33$ s).

A question that arises in this picture is what causes the electron and ion transport to converge to similar values at later times (Fig. 4). A possible answer is that the q -profiles evolve towards a similar shape, with sufficient negative shear to support relatively good electron confinement in both cases. In the fast ramp case it is likely that the increasingly strong off-axis sawteeth occurring after about $t \approx 0.3$ s weaken the initially strong reversal. In the slow ramp shot 112996, while TRANSP computes that the shear is becoming increasingly negative, at $t \approx 0.36$ s the TRANSP q -profile is still flatter than in 112989. However, in this shot a very slow (≈ 10 ms) reconnection-like event occurs at $t \approx 0.26$ s, which broadens the T_e profile, bringing it closer to that in 112989. This evolution is illustrated by T_e sensitive USXR measurements shown in Fig. 7. The slow evolution appears to be on the transport rather than the MHD time scale, possibly indicating a spontaneous transition to broader current profile and improved electron confinement.

Assuming the TRANSP and USXR indications for shear reversal with fast ramp, the above results suggest a positive correlation between improved electron confinement and *strong* negative magnetic shear s , in the low density NSTX L-modes. Indeed, the location of minimum χ_e in shot 112989 (Fig. 3) coincides with a region of maximal negative shear (s around -0.6 to -0.4) in Fig. 6a. This trend continues also at later times. The plasma with flat, or weakly reversed q -profile on the other hand, does not exhibit the early electron barrier.

The q -profile seems to also have an effect on ion transport. Thus, other conditions being comparable, shot 112996 in which the estimated q -profile is flat does not exhibit the pronounced χ_i decrease around $r/a \approx 0.4-0.5$ seen in shot 112989, in which the inferred q -profile is reversed. Also to be noted, in 112989 the region of reduced χ_i is at a different radius ($\approx q_{\text{min}}$) than that of reduced χ_e , suggesting different drives for electron and ion transport.

The above observations are further supported by data from fast ramp shots, but in which the beam was delayed in comparison with 112989, in order to allow more rapid current penetration and thus a narrower region of shear reversal. In these cases, χ_e is still reduced, but at a smaller radius, which is coincident with a negative shear region calculated by TRANSP. The ion barrier, although less pronounced, is also at a smaller radius in these plasmas.

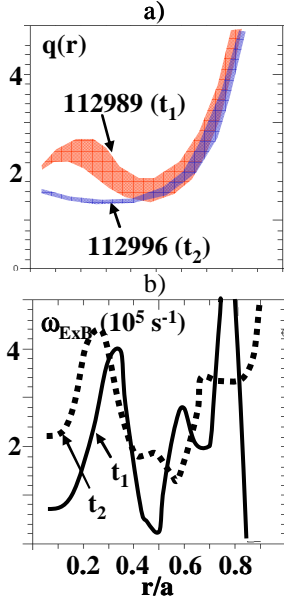


FIG. 6 a) TRANSP $q(r)$
b) ω_{ExB} using outboard un-smoothed profiles.

with the zero crossing at $s \approx -0.5$. Pending further confirmation of such shear values in shots like 112989, the inference would be that high $k_{\theta\rho_i}$ modes might play an important role for electron transport in the *gradient* region in NSTX. This inference also correlates with previous predictions for strong ETG drive in the gradient region of NSTX H-modes [8]. The ITG growth rate at mid-radius is also a few times less in 112989 versus 112996, in spite of the increased T_i gradient. This may be consistent with the q -profile influencing also the ion transport, as suggested by the present experiments. Lastly, the GS2 predictions for similar, large growth rates of ITG, TEM and ETG modes in both discharges at $r/a=0.65$ appear consistent with the large $\chi_{e,i}$ values existing in both shots at $r/a > 0.6$ (Fig.3a).

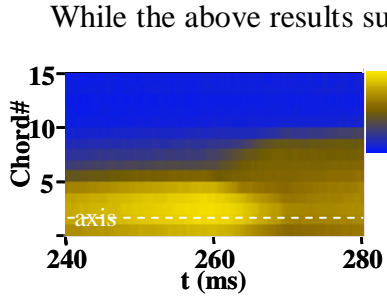


FIG. 7 'Spontaneous', slow broadening of $E > 1.4 \text{ keV}$ USXR profiles in 112996.

To guide the search for the possible drives behind electron transport in NSTX, linear gyrokinetic microstability calculations with the GS2 code [7] were performed for these plasmas. Although these calculations are local ('flux-tube' approximation), do not account for \mathbf{ExB} shear, and are restricted in their applicability at low magnetic shear, they can indicate where in the $k_{\theta\rho_i}$ spectrum a strong linear drive (growth rate) for instability exists, for given plasma gradients. The initial results at times t_1 and t_2 are summarized in Table I for core, mid-radius and outer radii.

There are several observations that can be made at this stage. First, shot 112989 which has reduced electron transport inside $r/a \approx 0.45$, has also much reduced instability drive for TEM and especially ETG modes in the same region, in spite of the stronger T_e gradient. A main reason for this prediction is the negative magnetic shear. This is shown in Fig. 8, with GS2 results of a numerical scan of the magnetic shear at $r/a \approx 0.5$ in a reduced χ_e discharge similar to 112989. The T_e gradient was kept fixed at the experimental value in this scan. As seen, increasingly negative shear suppresses the ETG growth rates,

While the above results suggest that the q -profile has a strong effect on transport in these plasmas, is difficult to assess the role of the \mathbf{ExB} shear through comparisons with the linear microstability predictions. In the core ($r/a \approx 0.25$) of both plasmas where the shearing rate is very high, the modes are stable or have low growth rates. In the gradient region ($r/a \approx 0.45$) of 112989 where the \mathbf{ExB} shear is low (due to the plateau in the rotation profile), the instability drive is already much reduced by the negative shear. Only in the gradient region of 112996 and at $r/a \approx 0.65$ for both shots, the growth rates of higher- k modes are comparable or exceed ω_{ExB} . Non-

Table I. GS2 growth rates (10^5 s^{-1}) of most unstable modes in the ITG, TEM and ETG range. Also shown the magnetic shear used in GS2 and the TRANSP \mathbf{ExB} shearing rate (10^5 s^{-1}).						
	Fast ramp 112989, $t_1=0.19 \text{ s}$			Slow ramp 112996, $t_2=0.25 \text{ s}$		
	$r/a=0.25$	$r/a=0.45$	$r/a=0.65$	$r/a=0.25$	$r/a=0.45$	$r/a=0.65$
s	-0.6	-0.45	2.3	-0.35	0.65	2.3
ITG	0.1	0.1	1.5	0.1	0.4	1.5
TEM	0.1	0.1	2.0	stable	1.8	3.8
ETG	stable	stable	7.8	stable	5.0	7.5
ω_{ExB}	2.5	0.5	2.2	4.5	1.8	2.5

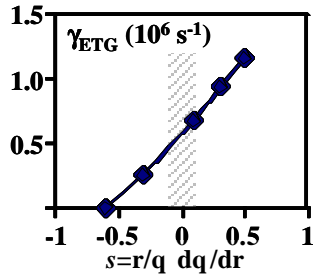


FIG. 8 GS2 growth rates of $k_{\perp} \rho_i \approx 35$ modes at $r/a = 0.4$, $t \approx 0.29$ s in shot 108213 as a function of magnetic shear. In the shaded area the GS2 prediction is less accurate.

linear gyrokinetic simulations are therefore underway to assess the role of \mathbf{ExB} shear in these plasmas. While neoclassical transport at very low B_p might eventually explain the flat T_i profile, it is not clear what drives the electron transport in the absence of measurable gradients.

Finally, density correlation length measurements performed in these discharges using microwave reflectometry indicate early in time large correlation lengths (\geq several cm), quite deep ($r/a \geq 0.3-0.5$) in the core of both the fast and slow ramp plasmas. The fast ramp case has nevertheless lower values. The spectral analysis indicates that these fluctuations may be associated with global magnetic fluctuations, including fast ion driven modes [4]. The possible effects of magnetic fluctuations on thermal transport in the ST are yet to be explored.

This work is supported by US DoE grant DE-FG02-99ER54523 at the Johns Hopkins University and by US DoE contract DE-AC02-76CH03073 at PPPL.

- [1] LEBLANC, B., et al., Nucl. Fusion **44** 2004 (513)
- [2] STUTMAN, D., et al., Phys. Plasmas **10** 2003 (4387)
- [3] MEYER, H., et al., Plasma Phys. Control. Fusion **46** 2004 (A291)
- [4] KAYE, S., et al., this conference.
- [5] STUTMAN, D., et al., Rev. Sci. Instrum. **74** 2003 (1982)
- [6] CHANG, Z., et al., Phys. Rev. Lett. **77** 1996 (3553)
- [7] KOTSCHENREUTHER, M., et al., Comput. Phys. Commun. **88** 1995 (128)
- [8] REDDI, M. H., et al., Proc. 31st EPS Conference on Plasma Physics, London 2004
- [9] CONNOR, J., et al., Nucl. Fusion **44** 2004 (R1)